

## RESEARCH OF THE FORCE VALUES DEPENDENCES IN HYDRO CYLINDERS OF THE MOBILE ELEVATING WORK PLATFORM ARTICULATED BOOM ON THE WORK POSITION AND LOAD WEIGHT

Nebojša ZDRAVKOVIĆ  
Milomir GAŠIĆ  
Mile SAVKOVIĆ  
Dragan PETROVIĆ

**Abstract:** The most common construction type of the mobile elevating work platform articulated boom with three segments has been analyzed in this paper. With some approximations taken, the paper gives a model for calculating the load transmission to the support on the vehicle chassis. Analytical dependences between force values in hydro cylinders and boom joints angles and geometric parameters of the boom sections and load weight were obtained. These dependences can be used as basis for design and optimization of the hydraulic installation parameters and hydraulic component selection. On the other hand, obtained functions enable adjustment of the geometric parameters of the boom and hydro cylinders anchor points in order to meet the requirements of the adopted hydraulic components.

**Key words:** mobile elevating work platform, articulated boom, hydro cylinder force

### 1. INTRODUCTION

A hoisting device that provides temporary access of men and equipment to hardly reachable spots, which are placed at certain heights (from a few meters to several tens of meters), is called hydraulic elevating platform. The most often in use are the hydraulic elevating platforms mounted on vehicle. Such machine is called Mobile Elevating Work Platform - MEWP, [5]. The advantage in exploitation often goes to hydraulic elevating platforms with articulating booms, which are typical representatives of structures with variable geometry (Fig.1) [3], in contemporary urban conditions, just because of configuration of terrain which has lot of obstacles such as street lights, traffic signs, advertising panels, trees, electric, phone and other public installations, parked cars and other objects.



Fig. 1. MEWP boom types: telescopic, articulating and combined boom type

The most important parameters of an elevating platform are, besides the lifting capacity, working height and horizontal reach (Fig.2).

Named application features distinct them from hoisting devices with permanent access to working places and put them into special purpose construction hoisters.

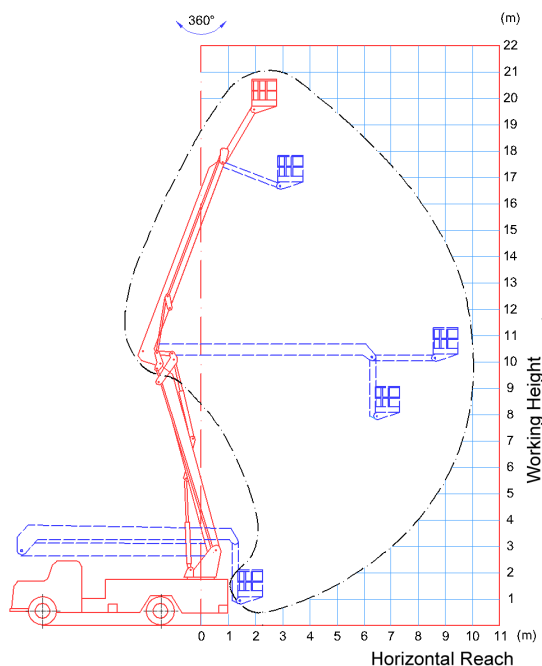


Fig.2. Working diagram of MEWP

## 2. APPROXIMATED CALCULATION MODEL

Boom having hinged sections is a complex mechanism, which is exposed to various loads such as load weight, self-weight of structure elements, dynamic loads at accelerating and decelerating and wind. It can be taken that on/off switching of hydraulic actuators is slow (gradual), by which the slow initiating and final movements of boom sections are realized. In this way, the dynamic loads are considerably decreased, that is the loads can be considered as quasi-static. If the wind is taken out of consideration as an exceptional type of load, calculation model of boom sections load is shown in Figure 5.

The sections' lengths and appropriate boom joint angles determine basket position within the work range (lifting height and horizontal reach). The angles defining basket position are those that sections enclose with constant directions:  $\alpha_1$  and  $\alpha_2$  are the angles that sections 1 and 2 enclose with the horizontal direction and  $\alpha_3$  is the angle that section 3 encloses with the vertical direction.

Every section is attached to the local (separate) movable coordinate system  $(\xi_i, \eta_i, \zeta_i, i=1,2,3)$ , at which the coordinate origin is placed at the joint connection with the previous section and  $\xi_i$  axes are perpendicular to the figure plane. At the section 1 support, that is the whole boom support, the global coordinate system  $AXYZ$  is set. In Fig. 4 there is shown the boom position at maximum joint angles that are:

$$\alpha_{1max} = 75^\circ, \alpha_{2max} = 70^\circ, \alpha_{3max} = 150^\circ.$$

There is a number of limitations for angles of sections 1, 2 and 3 during the operation, which are the result of acting of electrical and mechanical position limiting devices or structure limitations:

$$\alpha_1 + \alpha_2 \geq 15^\circ; \alpha_2 \leq \alpha_3 \leq \alpha_2 + 80^\circ; \alpha_3 \geq 0^\circ;$$

$$\alpha_{1max} = 75^\circ; \alpha_{2max} = 70^\circ; \alpha_{3max} = 150^\circ$$

Within basket position change, each boom section load is continually changing in the vertical  $XZ$  plane. In order to define loads, it is necessary to determine functional relations between all the forces that act on each section and joint angles  $\alpha_1$ ,  $\alpha_2$  and  $\alpha_3$ , as well as forces projections on local coordinate systems. Then, each section can be taken out of the structure and analyzed as separate carrier.

The sections weights are taken to act in their middle points at calculating the forces in relation to the named angles. Beside this, the model simplifying was done by reducing the influence of forces that act in leading bars on carrying sections, according to Figure 3.

Four bar linkage system, named the leading bars, provide the basket floor being horizontal and it is taken that they are approximately parallel with boom sections at distance

$l_0 \approx const$  for any boom position. On this basis, bar extension force is slightly changeable, so it can be, for the sake of simplifying, excluded from analysis. Work load consists of the basket and load mass  $m_T = m_k + m_Q$ , where  $m_k$  stands for basket mass and  $m_Q$  stands for mass of the operator and tools in the basket.

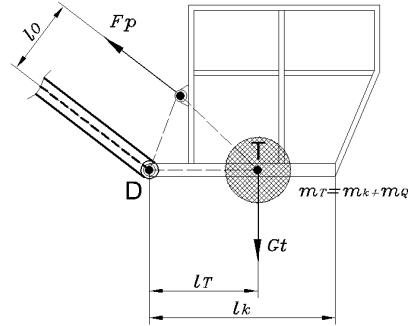


Fig. 3. Force in leading bars

Table 1. Constrained values of boom angles

$\alpha_1 [^\circ]$	0					
	45					
	75					
$\alpha_2 [^\circ]$	-60	-30	0	15	45	70
$\alpha_3 [^\circ]$	0÷20	0÷50	0÷80	15÷95	45÷125	70÷150

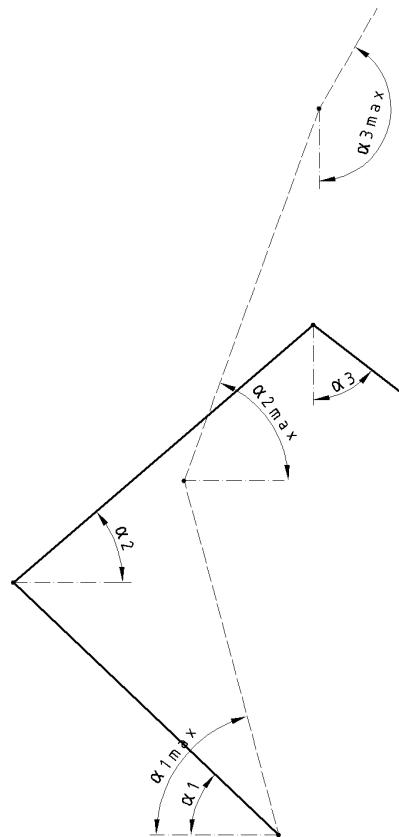


Fig. 4. Arbitrary and ultimate boom position

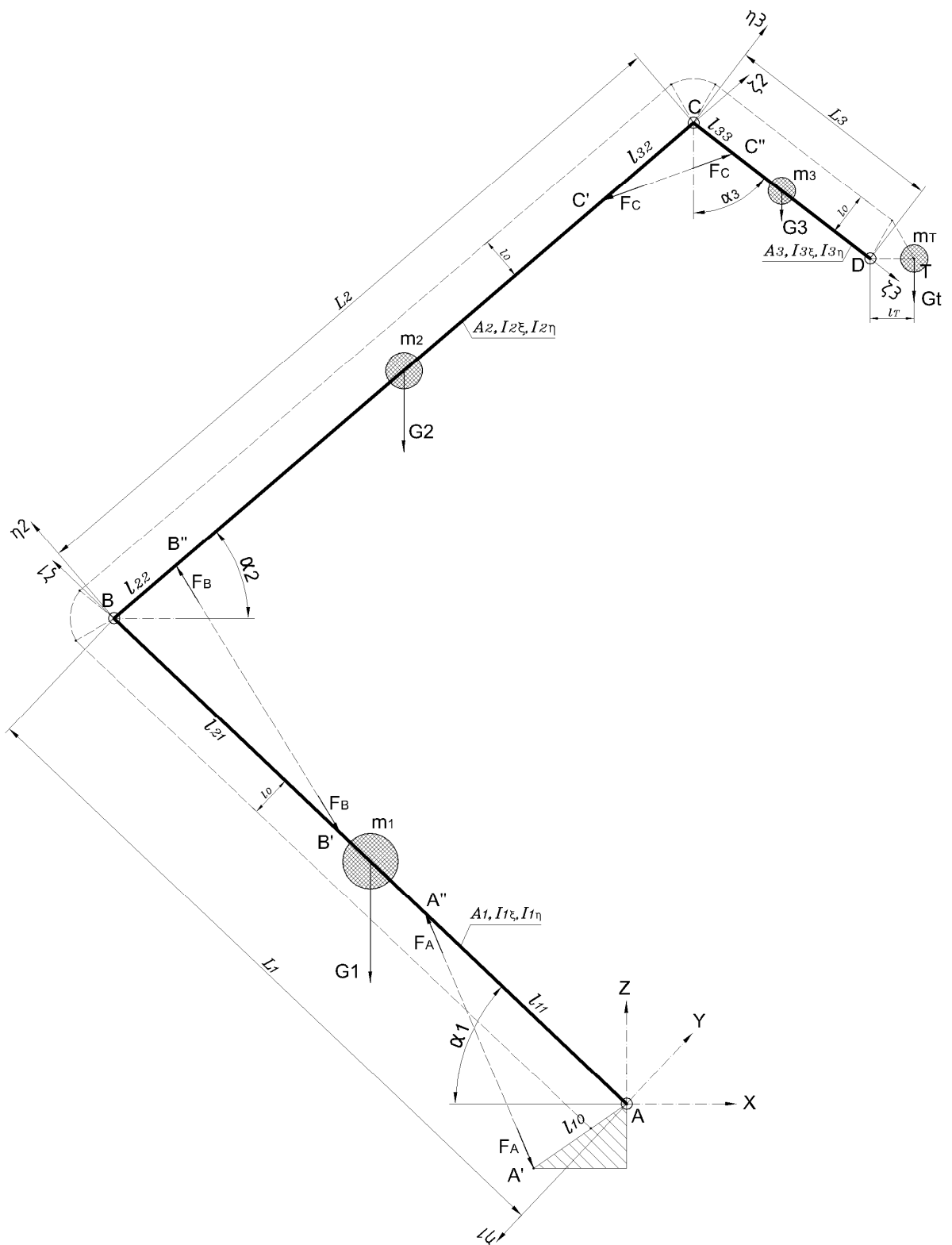


Fig. 5. Model for calculation of force values in hydro cylinders in relation to basket position

### 3. THE DETERMINATION OF HYDRO CYLINDERS' FORCE VALUES IN RELATION TO BASKET POSITION

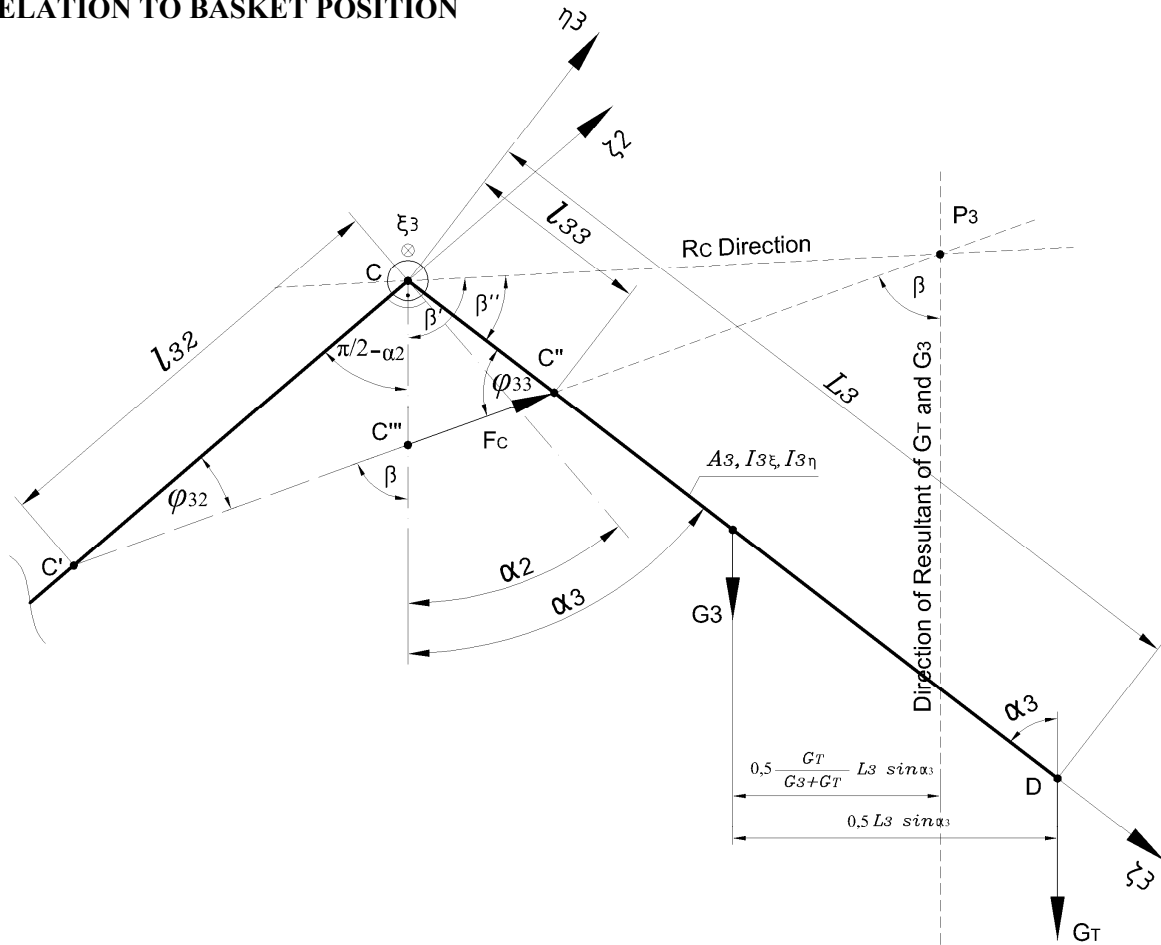


Fig. 6. Section 3 calculation model

We get force in hydro cylinder  $F_C$  from moment equation for  $C$  joint (Fig. 6):

$$G_T \sin \alpha_3 L_3 + G_3 \sin \alpha_3 \frac{L_3}{2} = F_C \sin \varphi_{33} l_{33} \quad (1)$$

The sine and cosine theorems are used for defining the angle  $\varphi_{33}$ , as well as the other angles which appear in consequent workflow. It shows that:

$$F_C = L_3 \sin \alpha_3 (G_T + 0,5G_3) \cdot \frac{\sqrt{l_{33}^2 + l_{32}^2 - 2l_{33}l_{32} \sin(\alpha_2 - \alpha_3)}}{l_{33}l_{32} \cos(\alpha_2 - \alpha_3)} \quad (2)$$

We get the reaction of section 2 on section 3 at joint  $C$  out of section 3 static equilibrium conditions:

$$R_c = \sqrt{(G_3 + G_T)^2 + F_C^2 - 2(G_3 + G_T)F_C \cos \beta} \quad (3)$$

All the forces should be projected on the local coordinate system  $C\xi_3\eta_3\zeta_3$ , in order to obtain the diagram of section 3 loads. Doing some angle transformations and equation substitutions, we get the expressions for the force in the hydro cylinder and section 3 loads:

$$F_c = L_3 \sin \alpha_3 (G_T + 0,5G_3) \cdot \frac{\sqrt{l_{33}^2 + l_{32}^2 - 2l_{33}l_{32} \sin(\alpha_2 - \alpha_3)}}{l_{33}l_{32} \cos(\alpha_2 - \alpha_3)} \quad (4)$$

$$F_{c\eta_3} = F_c \sin \varphi_{33} = \frac{L_3}{l_{33}} (G_T + 0,5G_3) \sin \alpha_3 \quad (5)$$

$$F_{c\xi_3} = F_c \cos \varphi_{33} = \frac{(G_T + 0,5G_3)l_3 [l_{33} - l_{32} \sin(\alpha_2 - \alpha_3)] \sin \alpha_3}{l_{33}l_{32} \cos(\alpha_2 - \alpha_3)} \quad (6)$$

$$R_{c\eta_3} = \left[ \left(1 - \frac{L_3}{l_{33}}\right)G_T + \left(1 - \frac{L_3}{2l_{33}}\right)G_3 \right] \sin \alpha_3 \quad (7)$$

$$R_{c\xi_3} = -(G_T + G_3) \cos \alpha_3 - \frac{(G_T + 0,5G_3)l_3 [l_{33} - l_{32} \sin(\alpha_2 - \alpha_3)] \sin \alpha_3}{l_{33}l_{32} \cos(\alpha_2 - \alpha_3)} \quad (8)$$

Section 2 calculation model is shown in Figure 7. Forces  $F_C$  and  $R_C$  are already defined, but now we take them in opposite directions.

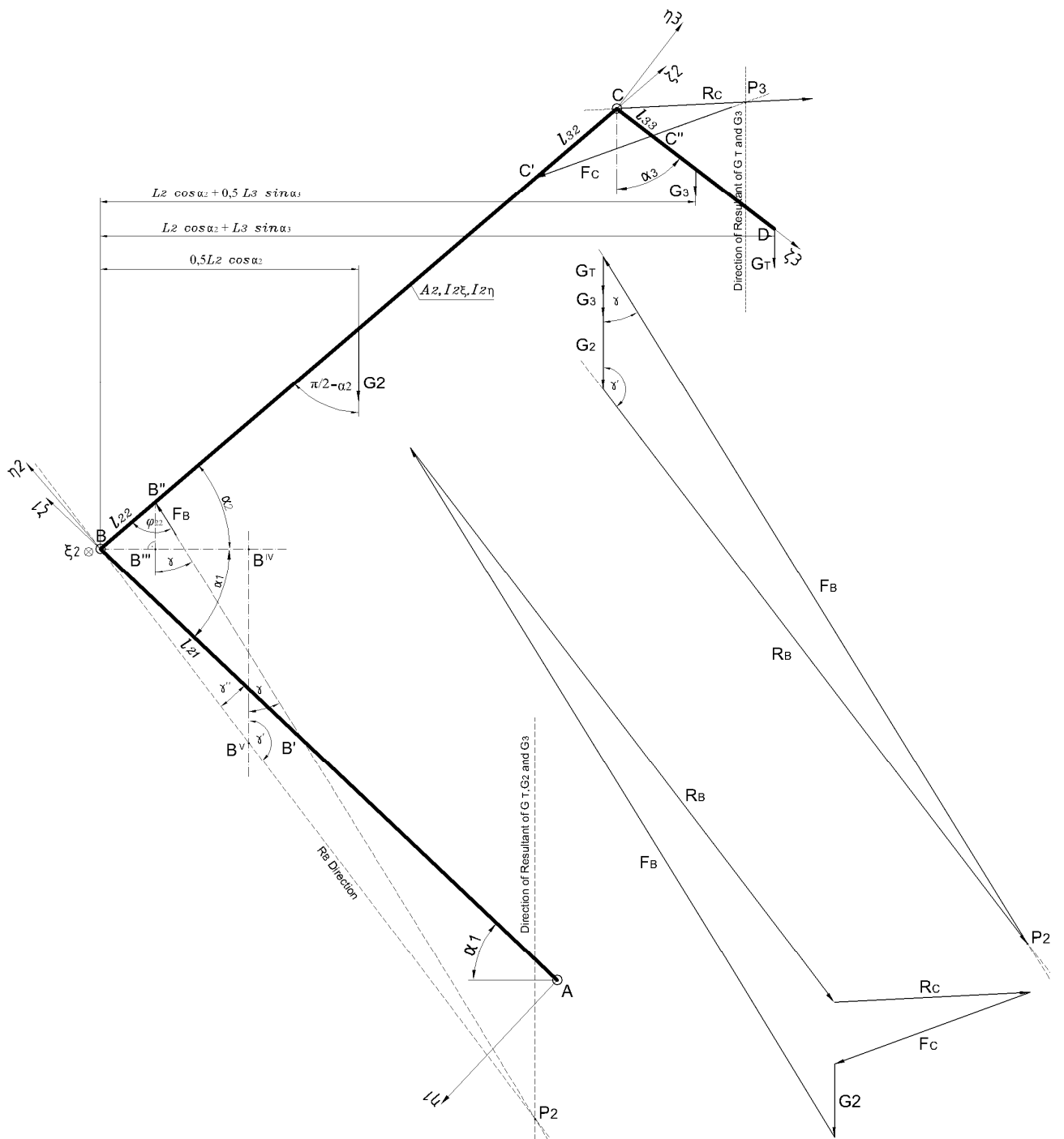


Fig.7. Section 2 calculation model

Force in hydro cylinder  $F_B$  we determine from moment equation for joint B :

$$l_2 \cos \alpha_2 (G_T + G_3 + 0,5G_2) + l_3 \sin \alpha_3 (G_T + 0,5G_3) = F_B \sin \varphi_{22} l_{22} \quad (9)$$

Reaction of section 1 on section 2 in joint B is:

$$R_B = \sqrt{(G_T + G_3 + G_2)^2 + F_B^2 - 2(G_T + G_3 + G_2)F_B \cos \gamma} \quad (10)$$

All the forces should be projected on the local coordinate system  $B\xi_2\eta_2\zeta_2$  in order to obtain the diagram of section 2 loads. After certain angle transformations and equation substitutions, we get the expressions for the force in the hydro cylinder and section 2 loads:

$$R_{c\eta_2} = -(G_3 + G_T) \cos \alpha_2 - \frac{l_3}{l_{32}} \sin \alpha_3 (G_T + \frac{G_3}{2}) \quad (11)$$

$$R_{c\zeta 2} = \frac{l_3 \sin \alpha_3 (G_T + \frac{G_3}{2})(l_{32} + l_{33} \sin(\alpha_3 - \alpha_2))}{l_{33} l_{32} \cos(\alpha_3 - \alpha_2)} - (G_3 + G_T) \sin \alpha_2 \quad (12)$$

$$F_{c\eta 2} = \frac{l_3}{l_{32}} (G_T + \frac{G_3}{2}) \sin \alpha_3 \quad (13)$$

$$F_{c\zeta 2} = -\frac{l_3 \sin \alpha_3 (G_T + \frac{G_3}{2}) [l_{32} + l_{33} \sin(\alpha_3 - \alpha_2)]}{l_{33} l_{32} \cos(\alpha_3 - \alpha_2)} \quad (14)$$

$$R_{c\eta 2} = -(G_3 + G_T) \cos \alpha_2 - \frac{l_3}{l_{32}} \sin \alpha_3 (G_T + \frac{G_3}{2}) \quad (15)$$

$$R_{c\zeta 2} = \frac{l_3 \sin \alpha_3 (G_T + \frac{G_3}{2})(l_{32} + l_{33} \sin(\alpha_3 - \alpha_2))}{l_{33} l_{32} \cos(\alpha_3 - \alpha_2)} - (G_3 + G_T) \sin \alpha_2 \quad (16)$$

$$F_{c\eta 2} = \frac{l_3}{l_{32}} (G_T + \frac{G_3}{2}) \sin \alpha_3 \quad (17)$$

$$F_B = \frac{\sqrt{l_{21}^2 + l_{22}^2 - 2l_{21}l_{22} \cos(\alpha_1 + \alpha_2)}}{l_{21}l_{22} \sin(\alpha_1 + \alpha_2)} \cdot [l_2 \cos \alpha_2 (G_T + G_3 + 0,5G_2) + l_3 \sin \alpha_3 (G_T + 0,5G_3)] \quad (18)$$

$$F_{B\eta 2} = \frac{l_2}{l_{22}} (G_T + \frac{G_2}{2} + G_3) \cos \alpha_2 + \frac{l_3}{l_{22}} (G_T + \frac{G_3}{2}) \sin \alpha_3 \quad (19)$$

$$F_{B\zeta 2} = \frac{l_{22} - l_{21} \cos(\alpha_1 + \alpha_2)}{l_{22}l_{21} \sin(\alpha_1 + \alpha_2)} \cdot [l_2 \sin \alpha_3 (G_T + \frac{G_2}{2} + G_3) \cos \alpha_2 + l_3 (G_T + \frac{G_3}{2}) \sin \alpha_3] \quad (20)$$

$$R_{B\eta 2} = (G_T + G_2 + G_3) \cos \alpha_2 - \frac{l_2}{l_{22}} \cos \alpha_2 (G_T + G_3 + \frac{G_2}{2}) - \frac{l_3}{l_{22}} \sin \alpha_3 (G_T + \frac{G_3}{2}) \quad (21)$$

$$R_{B\zeta 2} = (G_T + G_2 + G_3) \sin \alpha_2 - \frac{[l_2 \sin \alpha_3 (G_T + \frac{G_2}{2} + G_3) \cos \alpha_2 + l_3 (G_T + \frac{G_3}{2}) \sin \alpha_3]}{l_{21}l_{22} \sin(\alpha_1 + \alpha_2)} \cdot [l_{21}^2 + l_{22}^2 - 2l_{21}l_{22} \cos(\alpha_1 + \alpha_2)] \quad (22)$$

Section 1 calculation model is shown in Figure 8. Forces  $F_B$  and  $R_B$  are already defined, but now we take them in opposite directions. Force in hydro cylinder  $F_A$  we determine from moment equation for joint  $A$  :

$$l_1 \cos \alpha_1 (0,5G_1 + G_2 + G_3 + G_T) - l_2 \cos \alpha_2 (0,5G_2 + G_3 + G_T) - l_3 \sin \alpha_3 (0,5G_3 + G_T) = F_A l_{11} \sin \varphi_{11} \quad (23)$$

Reaction of boom support in joint  $A$  is obtained as follows:

$$R_A = \sqrt{(G_1 + G_2 + G_3 + G_T)^2 + F_A^2 - 2(G_1 + G_2 + G_3 + G_T)F_A \cos \delta} \quad (24)$$

All the forces should be projected on the local coordinate system  $A\xi_1\eta_1\zeta_1$  in order to obtain the diagram of section 1 loads. After certain angle transformations and equation substitutions, we get the expressions for the force in the hydro cylinder and section 1 loads:

$$R_{B\eta 1} = (G_T + G_3 + G_2) \cos \alpha_1 - \frac{l_2}{l_{21}} (G_T + G_3 + \frac{G_2}{2}) \cos \alpha_2 - \frac{l_3}{l_{21}} (G_T + \frac{G_3}{2}) \sin \alpha_3 \quad (25)$$

$$R_{B\zeta 1} = -(G_T + G_2 + G_3) \sin \alpha_1 + \frac{[l_{21} - l_{22} \cos(\alpha_1 + \alpha_2)]}{l_{21}l_{22} \sin(\alpha_1 + \alpha_2)} \cdot [l_2 \sin \alpha_2 (G_T + \frac{G_2}{2} + G_3) \cos \alpha_2 + l_3 (G_T + \frac{G_3}{2}) \sin \alpha_3] \quad (26)$$

$$F_{B\eta 1} = \frac{l_2}{l_{21}} (G_T + \frac{G_2}{2} + G_3) \cos \alpha_2 + \frac{l_3}{l_{21}} (G_T + \frac{G_3}{2}) \sin \alpha_3 \quad (27)$$

$$F_{B\zeta 1} = -\frac{l_{21} - l_{22} \cos(\alpha_1 + \alpha_2)}{l_{22}l_{21} \sin(\alpha_1 + \alpha_2)} \cdot [l_2 (G_T + \frac{G_2}{2} + G_3) \cos \alpha_2 + l_3 (G_T + \frac{G_3}{2}) \sin \alpha_3] \quad (28)$$

$$F_A = \frac{\sqrt{l_{10}^2 + l_{11}^2 - 2l_{10}l_{11} \cos(\alpha_1 + \alpha_0)}}{l_{10}l_{11} \sin(\alpha_1 + \alpha_0)} \cdot [l_1 \cos \alpha_1 (0,5G_1 + G_2 + G_3 + G_T) - l_2 \cos \alpha_2 (0,5G_2 + G_3 + G_T) - l_3 \sin \alpha_3 (0,5G_3 + G_T)] \quad (29)$$

$$F_{A\eta 1} = -\frac{l_1}{l_{11}} (G_T + \frac{G_1}{2} + G_2 + G_3) \cos \alpha_1 + \frac{l_2}{l_{11}} (G_T + \frac{G_2}{2} + G_3) \cos \alpha_2 + \frac{l_3}{l_{11}} \sin \alpha_3 (\frac{G_3}{2} + G_T) \quad (30)$$

$$F_{A\zeta 1} = \frac{l_{11} - l_{10} \cos(\alpha_1 + \alpha_0)}{l_{11}l_{10} \sin(\alpha_1 + \alpha_0)} \cdot [l_1 (G_T + \frac{G_1}{2} + G_2 + G_3) \cos \alpha_1 - l_2 (G_T + \frac{G_3}{2}) \cos \alpha_2 - l_3 \sin \alpha_3 (\frac{G_3}{2} + G_T)] \quad (31)$$

$$R_{A\eta 1} = \frac{l_1}{l_{11}} (G_T + \frac{G_1}{2} + G_2 + G_3) \cos \alpha_1 - \frac{l_2}{l_{11}} (G_T + \frac{G_2}{2} + G_3) \cos \alpha_2 - \frac{l_3}{l_{11}} (G_T + \frac{G_3}{2}) \sin \alpha_3 - (G_T + G_1 + G_2 + G_3) \cos \alpha_1 \quad (32)$$

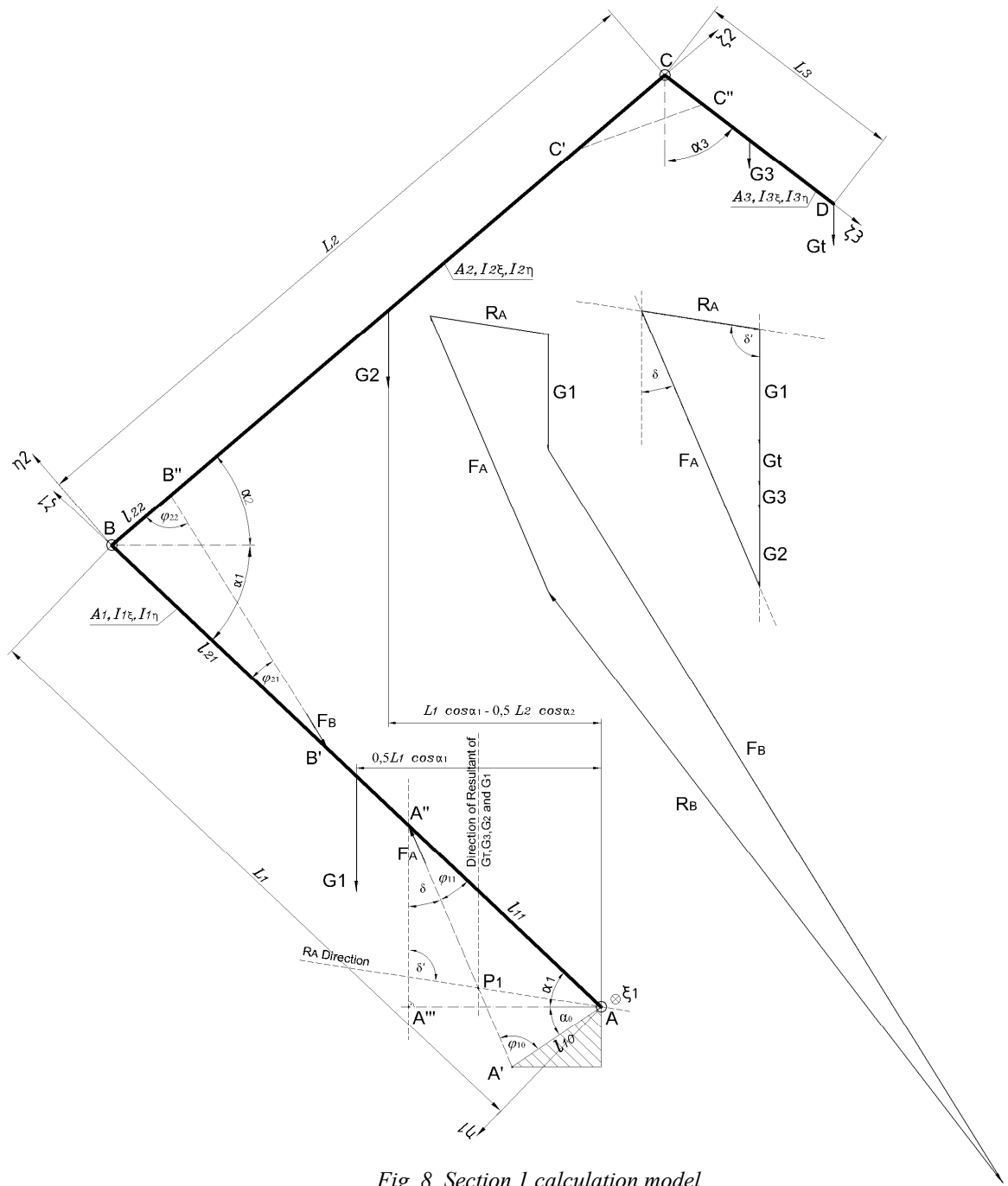


Fig. 8. Section 1 calculation model

$$\begin{aligned}
 R_{A\zeta 1} = & (G_1 + G_2 + G_3 + G_T) \sin \alpha_1 - \\
 & \frac{l_{11} - l_{10} \cos(\alpha_1 + \alpha_0)}{l_{11} l_{10} \sin(\alpha_1 + \alpha_0)} \cdot [-l_2(G_T + \frac{G_2}{2} + G_3) \cos \alpha_2 + \\
 & + l_1(G_T + \frac{G_1}{2} + G_2 + G_3) \cos \alpha_1 - l_3 \sin \alpha_3 (\frac{G_3}{2} + G_T)] \quad (33)
 \end{aligned}$$

The diagrams of some of the forces and their projections on local movable axes in relation to  $\alpha_1$ ,  $\alpha_2$  and  $\alpha_3$  angles are shown in Figures 9 and 10. The following numerical values for diagram plotting purpose were used:

$$\begin{aligned}
 L_1 = & 7602 \text{ mm}, L_2 = 8210 \text{ mm}, L_3 = 2400 \text{ mm}, l_{33} = 540 \text{ mm}, \\
 l_{32} = & 1288 \text{ mm}, l_{22} = 876 \text{ mm}, \alpha_0 = 35^\circ, \\
 l_{21} = & 3361 \text{ mm}, l_{11} = 2987 \text{ mm}, l_{10} = 1215 \text{ mm}, \\
 G_1 = & 15 \text{ kN}, G_2 = 10 \text{ kN}, G_3 = 4 \text{ kN}, G_T = 5 \text{ kN}
 \end{aligned}$$

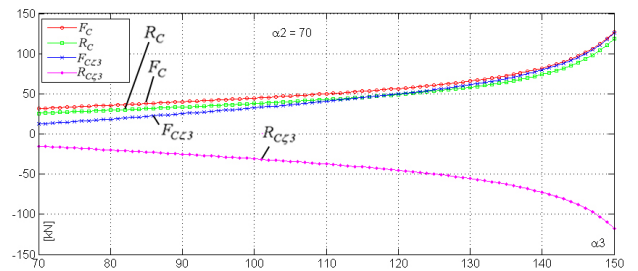


Fig. 9. Diagrams  $F_C$ ,  $R_C$ ,  $F_{C\zeta 3}$  and  $R_{C\zeta 3}$  for  $\alpha_2 = 70^\circ$  at angle  $\alpha_3$  change

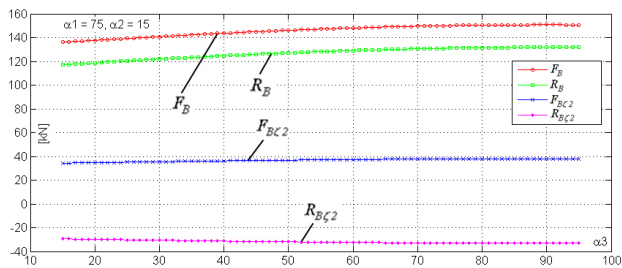


Fig. 10. Diagrams  $F_B, R_B, F_{B\zeta 2}$  and  $R_{B\zeta 2}$  for  $\alpha_1 = 75^\circ$  and  $\alpha_2 = 15^\circ$  at angle  $\alpha_3$  change

#### 4. CONCLUSION

By analysing the MEWP articulated boom, the functional dependences of forces in hydro cylinders were obtained. The tracking of forces in all MEWP hydrocylinders was enabled. Analytical forms also open a possibility for insight into the influence of boom's geometric parameters variations, such as anchor points' positions and segments' lengths, on the pistons' forces values. Decreasing of these forces would lead to optimization of the hydro cylinders and boom's design.

#### REFERENCES

- [1] JERMAN, B., KRAMAR, J. (2008) *A study of the horizontal inertial forces acting on the suspended load of slewing cranes*, International Journal of Mechanical Sciences, Volume 50, Issue 3, March 2008, pp 490-500
- [2] JERMAN, B., PODRŽAJ, P., KRAMAR, J. (2004) *An investigation of slewing-crane dynamics during slewing motion—development and verification of a mathematical model*, International Journal of Mechanical Sciences, Volume 46, Issue 5, May 2004, pp 729-750
- [3] BOŠNJAK, S., ZRNIĆ, N., DRAGOVIĆ, B. (2009) *Dynamic Response of Mobile Elevating Work Platform under Wind Excitation*, Strojniški vestnik - Journal of Mechanical Engineering, Vol. 55, No. 2 (2009), pp 104-113. ISSN 0039-2480.
- [4] GAŠIĆ, M., SAVKOVIĆ, M., BULATOVIĆ, R., PETROVIĆ, R. (2010). *Optimization of a pentagonal cross section of the truckcrane boom using Lagrange's multipliers and differential evolution algorithm*, Meccanica - An International Journal of Theoretical and Applied Mechanics, ISSN 1572-9648 (electronic version), ISSN 0025-6455 (print version), DOI 10.1007/s1 1012-010-9343-7
- [5] RADOIČIĆ G. (2006) *Experimental testing of vibro-comfort on mobile elevating work platform*, Research and Design in Commerce & Industry, No. 11, year IV(2006), pp 25-35, ISSN 1451-4117.

#### CORRESPONDENCE



Nebojša Zdravković, Ass. M.Sc. Eng.  
University of Kragujevac  
Faculty of Mechanical Engineering  
Kraljevo  
Dositejeva 19, 36000 Kraljevo, Serbia  
zdravkovic.n@mfkv.kg.ac.rs



Milomir Gašić, Prof. D.Sc. Eng.  
University of Kragujevac  
Faculty of Mechanical Engineering  
Kraljevo  
Dositejeva 19, 36000 Kraljevo, Serbia  
gasic.n@mfkv.kg.ac.rs



Mile Savković, Prof. D.Sc. Eng.  
University of Kragujevac  
Faculty of Mechanical Engineering  
Kraljevo  
Dositejeva 19, 36000 Kraljevo, Serbia  
savkovic.m@mfkv.kg.ac.rs



Dragan Petrović, Prof. D.Sc. Eng.  
University of Kragujevac  
Faculty of Mechanical Engineering  
Kraljevo  
Dositejeva 19, 36000 Kraljevo, Serbia  
petrovic.n@mfkv.kg.ac.rs